ELSEVIER

S0032-3861(96)00327-8

Polymer Vol. 37 No. 21, pp. 4773–4785, 1996
Copyright © 1996 Elsevier Science Ltd
Printed in Great Britain. All rights reserved
0032-3861/96/$15.00 + 0.00

Molecular modelling simulation of gas transport in amorphous polyimide and poly(amide imide) membrane materials

D. Hofman*, J. Ulbrich, D. Fritsch and D. Paul
GKSS Research Center Geesthacht, Institute of Chemistry, Kantstrasse 55, D-14513 Teltow, Germany
(Received 19 October 1995; revised 12 January 1996)

Molecular dynamics (MD) simulations were used to investigate the transport of different gases in a poly(amide imide) (PAI) and two polyimides (PI1 and PI2). The agreement between measured and simulated average diffusion coefficients (D) was acceptable. There was, however, a considerable scattering of the D values for the individual simulated gas molecules. While MD simulations are still not an ideal tool for the quantitative prediction of gas permeation properties of polymers, these methods can be used to obtain a better insight about the gas transport mechanism. Transport of small molecules occurs by jumps between individual sections of the free volume (holes) through temporarily open channels. The main difference between the PAI and the two polyimides is broader and slightly more permanent channels in the case of the PAI. Solubility investigations using the Widom method revealed a predominantly Henry sorption mechanism for hydrogen, a dual-mode sorption with a high degree of Langmuir-type immobilization for oxygen and nitrogen. Copyright © 1996 Elsevier Science Ltd.

(Keywords: molecular modelling; gas diffusion; polyimides)

INTRODUCTION

Up to now the development of new polymers for gas separation using amorphous polymer membranes has been a very laborious process, including trial and error procedures. A better understanding of the gas transport mechanism of gases in polymers on a molecular level is clearly needed. Furthermore, quantitative predictions of gas separation properties from the repeat unit composition of amorphous polymers would be very useful. Over the past 5 years, molecular modelling has proved itself to be a useful tool for these purposes. This simulation technique has become a widely used method for the investigation of the molecular structure of amorphous polymers and the diffusion of small gas molecules through these materials. Most of these simulations deal with flexible-chain polymers composed of rather simple (model) repeat units, among them poly(dimethyl siloxane) (PDMS) and poly(isobutylene) (PIB)[1–9], or polymers such as poly(ethylene) (PE) or poly(propylene) (PP)[10–13]. A more general overview is given elsewhere[14,15]. A 200 ps molecular dynamics (MD) simulation of gas transport in stiff-chain polyimide polymer models made from about 1200 atoms was reported by Smit *et al.*[16].

The investigations mentioned show that the diffusion of small gas molecules through amorphous polymers consists of two different modes of motion. Over relatively long periods of time (typically a few 100 ps) the gas molecules simply 'explore' distinct holes in the free volume. Thereby they are reflected by the thermally vibrating polymer matrix about every 1–2 ps. Eventually, a channel to an adjacent hole is opened for a short time, which under favourable circumstances allows permeating molecules to jump from one hole to the next. The diffusion coefficient is completely determined by the jump events. MD simulations are successful only when detailed atomistic models are used for both the polymer matrix and the gas molecules, and if the thermal vibrations of the polymer matrix are taken into consideration.

In this paper, results of molecular modelling investigation of gas transport in three relatively stiff membrane polymers are presented. The polymers are a poly(amide imide) (PAI) and two polyimides (PI1 and PI2). These materials are of interest for the separation of O_2/N_2 and H_2/N_2. In particular, PI1 is among the polymers with the highest gas permeabilities found so far for polyimides see *Table 1* and Fritsch *et al.*[19]. In the case of the PAI only the transport of hydrogen is considered, because with this polymer the observed diffusion coefficients for O_2 and N_2 are too small to permit a successful MD simulation within a reasonable time. The O_2 and N_2 transport could, however, be simulated for the polymers PI1 and PI2.

It is a long-term aim of MD simulations of membrane transport to predict membrane properties quantitatively. To illustrate the respective present possibilities, PI2, which has not yet been synthesized, was included in this study. PI2 is a modification of PI1 carrying an additional trimethylphenylene group per repeat unit (*Figure 1*).

EXPERIMENTAL

Materials

PI1 was synthesized according to a procedure first

* To whom correspondence should be addressed

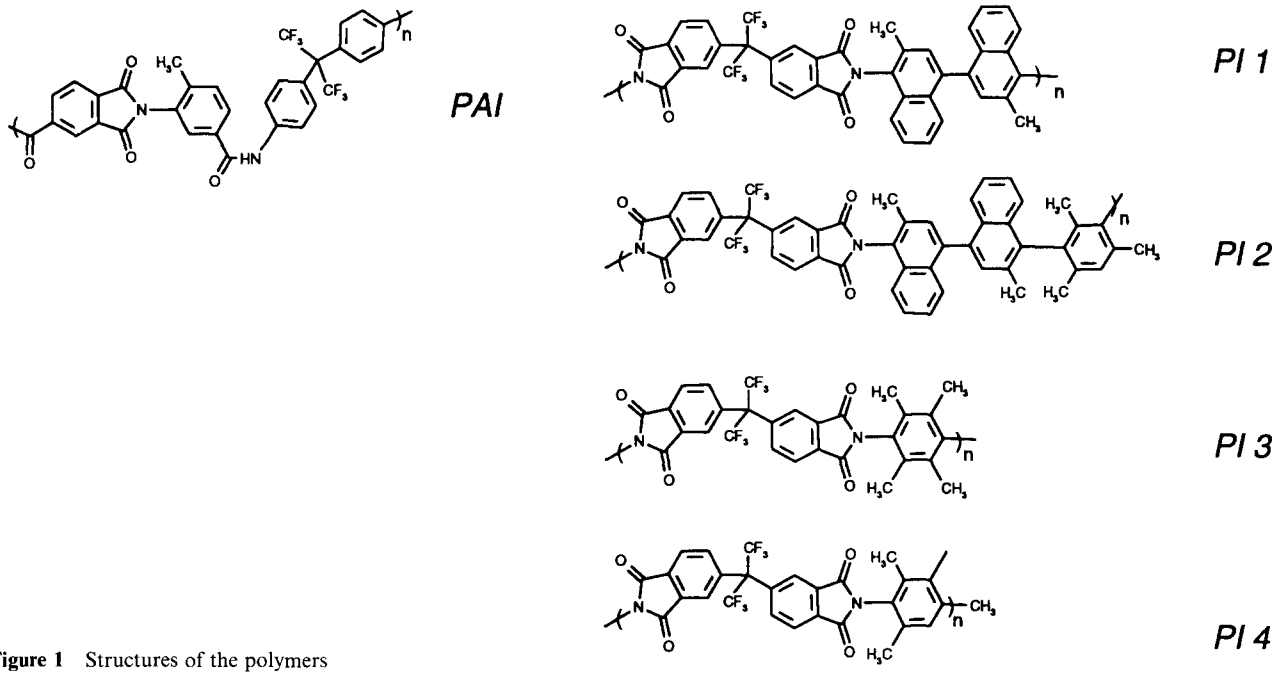

Figure 1 Structures of the polymers

described by Hayes [18], while the PAI syntheses is described by Fritsch and Peinemann[19]. Films (thickness 40–100 μm) were prepared from tetrahydrofuran (THF) solutions. After solvent evaporation, the films were immersed in methanol overnight and dried in a vacuum (< 1 mbar) at 383 k for 16 h. *Figure 1* and *Table 1* give the structures and measured gas permeation data. *Table 1* also reports data for the two polyimides PI3 and PI4[18] measured for films prepared under the same conditions as mentioned above. PI3 and PI4 are structurally very similar to PI1 and PI2. Thus the following discussion of molecular simulation results should also be qualitatively valid for PI3 and PI4.

The synthesized polymers PAI and PI1 are basically amorphous, as indicated by wide-angle X-ray scattering (WAXS) measurements and differential scanning calorimetry (d.s.c.).

Molecular modelling software and hardware

The models of molecular packing were constructed and simulated by means of the InsightII/Discover Software of Biosym Technologies*. The Biosym consistent valence force field (cvff)[17,20–22] was applied for all static and dynamic simulations. The calculations were performed on two IBM RS 6000 workstations (models 340 and 3BT) and on the CRAY C916 of the Deutsches Klimarechenzentrum (DKRZ) in Hamburg, FRG.

Force field

A detailed description of the cvff can be found in the *Discover User Guide*[20]. This force field is parametized for a large class of organic molecules, allowing it to be applied to many bio- and artificial polymers. This force field can be used to calculate and minimize the energy of a simulated system. Furthermore, it is possible to calculate the forces acting on each atom of a model polymer, which can then be utilized to solve Newton's equations of motion for MD simulations.

Model and simulation details

In a first stage the repeat units were built (see *Figure 1* and *Table 2*). Then chains containing between 1922 and 3202 atoms were made from these repeat units. The number of repeat units seems to be rather small in all cases; however, the simulated chains contain a sufficient number of flexible bonds (e.g. 180 for PI1, 270 for

Table 1 Gas permeation data for the experimentally available polymers including two reference materials, PI3 and PI4. P is the permeability measured in barrers (1 barrer = 1×10^{-10} cm^3 (STP) cm cm^{-2} s^{-1} cmHg^{-1}. D is the diffusivity in $10^{-7} \times cm^2/s^{-1}$

Polymer	PN_2	PO_2	PH_2	PHe	PCH_4	PCO_2
PAI	0.5	1.9	14.2	–	–	–
PI1	61.4	213	812	449	71.8	1.4
PI3	56.6	213	849	522	53.1	1.2
PI4	48.8	159	622	415	44.6	0.6

Polymer	PO_2/PN_2	PHE/PN_2	PH_2/PN_2	PCO_2/PN_2	PCO_2/PCH_4
PAI	3.8	–	28.4	–	–
PI1	3.47	7.30	13.2	22.0	18.9
PI3	3.77	9.23	15.0	20.4	21.8
PI4	3.25	8.50	12.8	13.1	14.3

Polymer	DN_2	DH_2	DO_2	DCH_4	DCO_2
PAI	0.1	9.4	0.3	–	–
PI1	2.8	–	7.4	0.7	3.0
PI3	4.0	–	7.7	0.45	2.5
PI4	2.4	–	5.2	0.51	2.3

* The computational results were obtained from software programs supplied by Biosym Technologies of San Diego, USA. Static and dynamic calculations were done with the Discover program, using the cvff. The amorphous packings were obtained with the help of the Amorphous Cell module. Some data evaluations were performed and graphically displayed utilizing the InsightII molecular modelling system

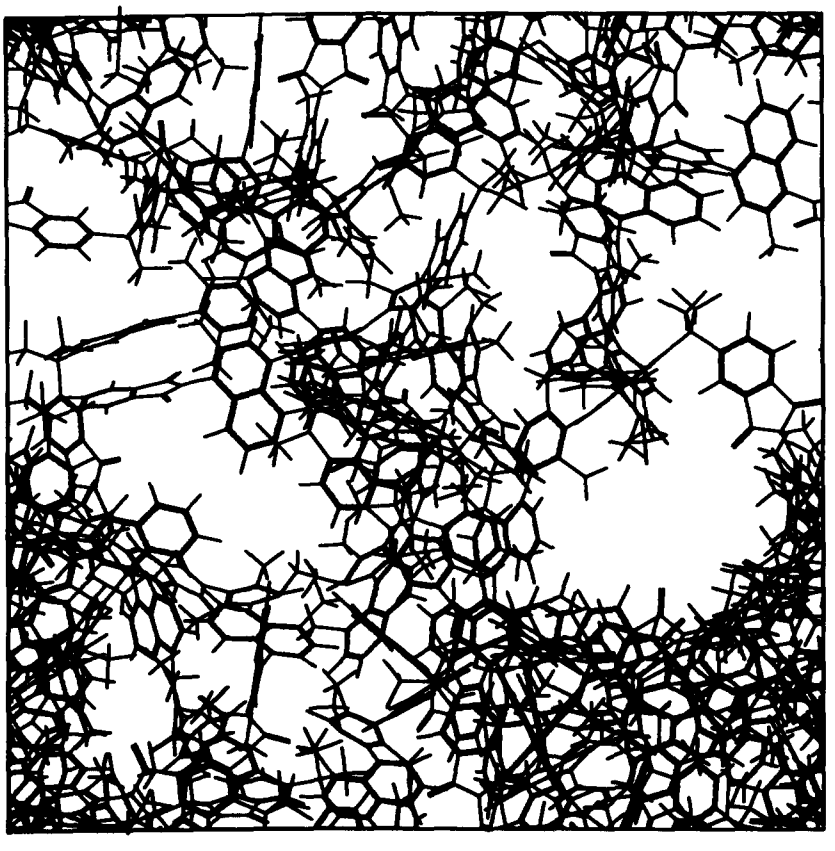

Figure 2 Initial-guess amorphous chain packing for PI2

Table 2 General packing parameters

Packing number	Type of polymer	Number of repeat units	Number of atoms in the polymer packing	Number and types of permeate molecules	Average periodic box dimensions after system refinement (nm)	Measured density (g cm^{-3})	Average simulated density after system refinement (g cm^{-3})
1	PAI	30	1922	1 H_2	2.8212	1.395	1.383
2	PAI	30	1922	1 H_2	2.8199	1.395	1.385
3	PAI	30	1922	5 H_2	2.8217	1.395	1.382
4	PAI	50	3202	5 H_2	3.3476	1.395	1.380
5	PI1	37	2777	5 O_2 + 5 N_2	3.2935	1.274	1.255
6	PI2	30	2822	5 O_2 + 5 N_2	3.2199	NA	1.273

NA, not available

the 30-repeat unit PAI and 450 for the 50-repeat unit PAI). It should be noted that it is the number of flexible bonds in a chain and not just the number of repeat units that is a decisive parameter for the achievable quality of an amorphous packing made from a chain. These chains were subjected to a static structure optimization via a steepest-descent energy minimization until the maximum energy gradient at any atom was below 10 kJ mol^{-1} nm^{-1}.

In a second stage the amorphous cell module of the InsightII software was utilized to obtain an initial-guess filling of periodic boxes with chain segments. For this purpose the Theodorou–Suter approach[23,24] with some modifications[25] was used. The polymer chains are grown at 303 K under cubic periodic boundary conditions. The volume of the basic cell is chosen in such a way that the experimentally obtained macroscopic density is reproduced when all the atoms of the simulated chain are placed in that cube. In the case of PI2 the measured density of PI1 was considered in this early stage of the simulation. The gas molecules, whose diffusion through the respective polymer is to be modelled, are inserted during the same procedure at positions which are energetically feasible. Another very important condition to be met by amorphous packing procedures is the reproduction of the conformational statistics of the backbone dihedral angles present in a real amorphous polymer of the given type. Here, because of the complex structure of the utilized repeat units, it is not possible to rely on standard textbook[26] data from the rotational isomeric state (RIS) theory. Instead, an automatic systematic conformational search is performed to

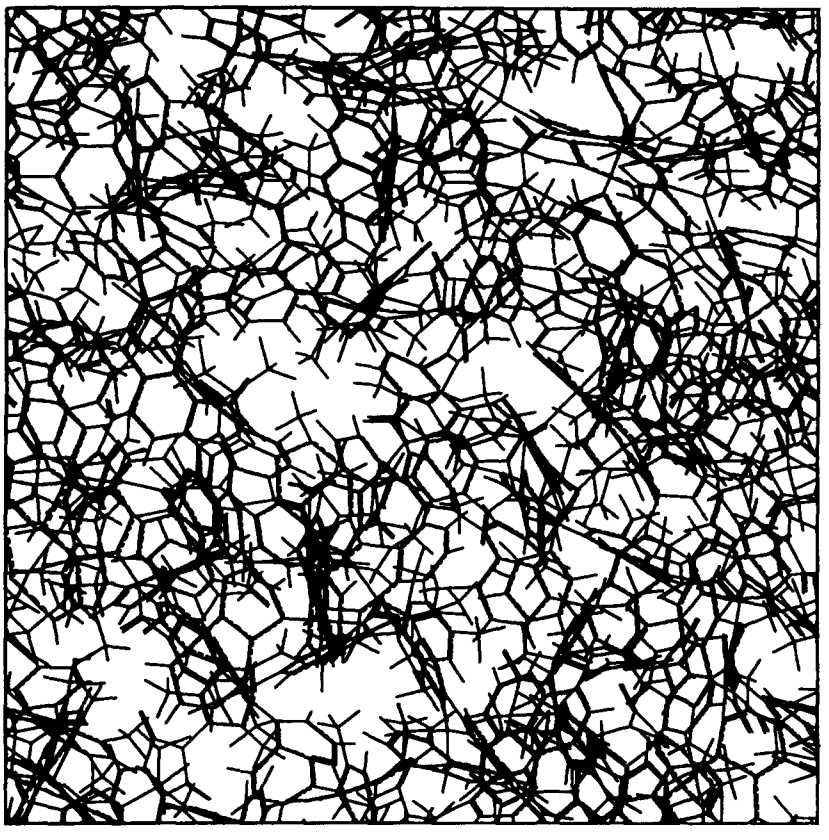

Figure 3 PI2 packing after the refinement stage

determine the Boltzmann probabilities for all relevant conformational states (conformations of minimum energy) of the flexible bonds in a chain. During the stepwise growth of a chain into the space, images of the constituent segments are transformed in the basic volume element. Then an additional criterion for the acceptance of an added flexible backbone bond (with its attached side-groups) is to avoid excessive atomic overlap in the packed cell. Further details of the Biosym amorphous packing algorithm can be found in the *Polymer User Guide*[25]. It should be noted that here just one chain was used for the packing in each case, considerably reducing the effect of chain ends on the simulation. In the literature, the use of several shorter chain segments is also reported[8,10,16].

For the sake of efficiency of the packing algorithm, it is not possible to meet all the mentioned criteria to the same extent. The method used here emphasizes the density and the conformation angle distribution criteria at the cost of relatively severe interatomic overlaps. A typical result of such an initial-guess packing is depicted in *Figure 2*. It is characterized by a considerable number of unrealistically large holes side by side with regions of too densely packed chain segments. It is, therefore, necessary to refine (equilibrate) this initial packing in a third stage. Sequences of static structure optimizations and MD simulations combined with force field parameter scaling are utilized for this purpose. The following conditions were used in all cases:

(i) Minimum image periodic boundary conditions to make the systems numerically tractable and to avoid artificial symmetry effects

Table 3 Force field scaling factors for amorphous packing refinement procedure A

Number of stage	Scaling factor for conformation terms	Scaling factor for non-bond terms
1	0.001	0.001
2	0.1	0.001
3	1	0.001
4	1	0.1
5	1	1

(ii) A cut-off distance for all non-bond interactions of 1.35 nm with a smooth switching function being used for all interatomic distances between 1.0 and 1.2 nm. At 1.2 nm the non-bond interactions between two atoms are considered to be exactly zero. The distance interval between 1.2 and 1.35 nm is necessary as a buffer because the list of atom pairs for which the non-bond interaction energy needs to be calculated is updated only about every 20 time steps. This considerably speeds up the simulations. The buffer width then accounts for the fact that during 20 time steps some additional pairs of atoms might decrease their distances below 1.2 nm.
(iii) A simulation time step of 1 fs.
(iv) The Berendsen method[27] of temperature and pressure bath coupling with a coupling constant of 100 fs to stabilize the intended system temperature and pressure during MD runs.

For the basic equilibration, a constant particle number, volume and temperature (NVT) ensemble was

Table 4 Specific force field parameters for amorphous packing refinement procedure B

Number of stage	Scaling factor for conformation terms	Type of non-bond terms	Scaling factor for *van der Waals* radii
1	0.001	Quartic	0.5
2	0.1	Quartic	0.5
3	1	Quartic	0.5
4	1	6–12 Lennard-Jones	1
5	1	6–12 Lennard-Jones	1

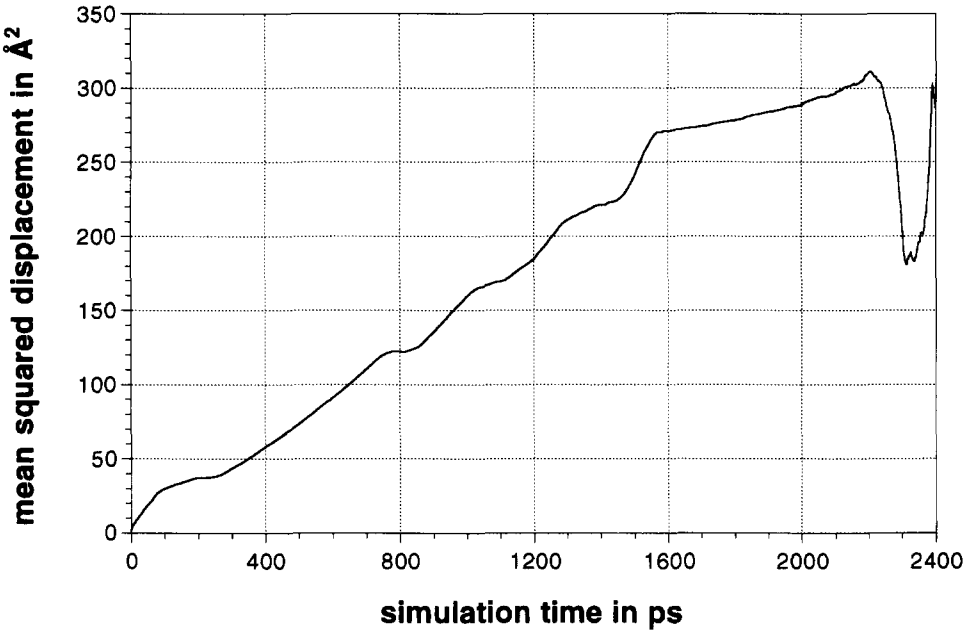

Figure 4 Plot of mean squared displacement *s versus* simulation time *t* for oxygen O6 in PI2

chosen. Two specific refinement procedures were utilized: method A relies on the original non-bond terms of the force field, and uses just a scaling of the conformation energy and non-bond energy terms as shown in *Table 3*. This means that, first, both terms are scaled down to very low values, which introduces a lot of extra mobility in the simulated chain packing. Then the system is gradually brought back to the real force field parameters. Method B resembles that described by Theodorou and Suter[23], and uses in the beginning a soft-sphere (no attraction) non-bond potential with a quartic repulsive term and down-scaled van der Waals radii. Further details are shown in *Table 4*.

The periodic volume element looks more homogeneously filled with chain segments after either one of these refinement procedures (see *Figure 3*). Then for the PAI and PI1 a 1 bar constant pressure NPT MD run was performed in each case to check whether the refined system met the density criterion at normal pressure conditions. Unfortunately, after this first refinement the density is usually 10–20% lower than the measured value. This indicates that there are still unrealistic tensions in the simulated packing that need further equilibration. The use of cut-off corrections for the pressure did not result in significant density changes). This was usually performed via several cycles of:

(1) an NPT MD run at $1 \times 10^4 - 5 \times 10^4$ bar to bring the system density well above the measured value;
(2) equilibration of the resulting structure with one of the procedures mentioned above;
(3) a 1 bar NPT run.

In a few cases some simulated annealing was also necessary. At the end it was always possible to get the system to a simulated density with a maximum deviation of −1.5% from the measured value (see *Table 2*). This density value was then stable under 1 bar conditions over the whole following MD production run. Because PI2 is not yet synthesized, the density equilibration procedure just described was applied more often than for the PAI and PI1 packings. This should ensure that the density given in *Table 2* for this material is close to the value expected for PI2.

After the complete system refinement, the movement of the included small H_2, O_2 or/and N_2 molecules through the thermally vibrating polymer matrix was followed by an NPT MD production run at 1 bar and 303 K. The periodic boundary, cut-off and temperature and pressure bath conditions were chosen as for the case of the refinement procedures mentioned above. The length of the simulations was between 1 and 2.5 ns, which was considerably (up to 10 times) longer than in the modelling of CO_2 diffusion in polyimides discussed by Smit *et al.*[16]. This fact just reflects the increase of the available hardware performance over the last 3 years.

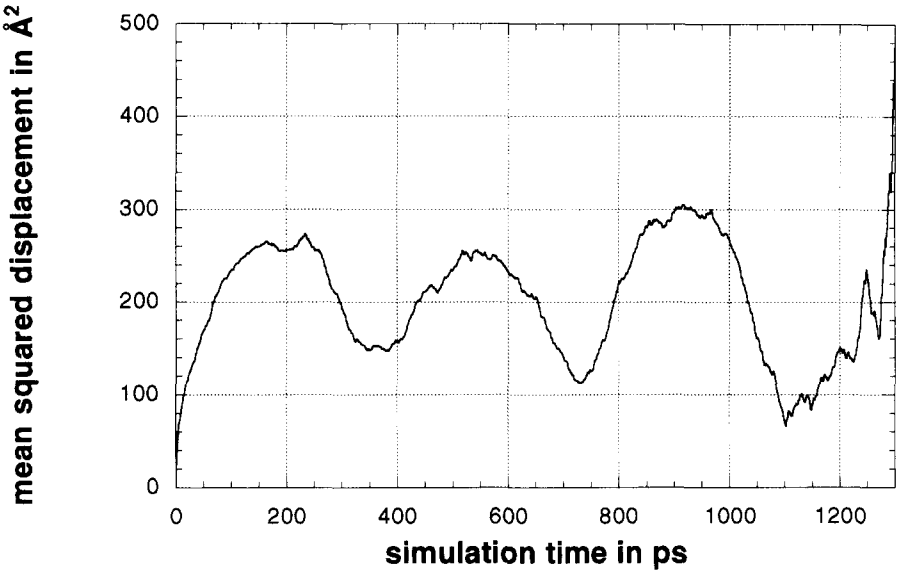

Figure 5 Plot of mean squared displacement s *versus* simulation time t for hydrogen H5 in the PAI

Table 5 Experimental and simulated constants of diffusion

Packing number	Type of polymer	Type and number of simulated gas molecule	Measured constant of diffusion (10^{-7} cm^2 s^1)	Simulated constant of diffusion (10^{-7} cm^2 s^{-1})
1	PAI	H 1	9.40	13.6
2	PAI	H 2	9.40	13.0
3	PAI	H 3	9.40	0[a]
		H 4	9.40	230[b]
		H 5	9.40	120[b]
		H 6	9.40	27.0
		H 7	9.40	0[a]
4	PAI	H 8	9.40	21.7
		H 9	9.40	0[a]
		H10	9.40	200[c]
		H11	9.40	880[c]
		H12	9.40	880[c]
5	PI1	N1	2.8	5.2
		N2	2.8	8.8
		N3	2.8	7.8
		N4	2.8	0[a]
		N5	2.8	40
5	PI1	O 1	7.4	26.9
		O 2	7.4	39.5
		O 3	7.4	0[a]
		O 4	7.4	14.8
		O 5	7.4	81
6	PI2	N 6	NA	13.1
		N 7	NA	0[a]
		N 8	NA	26.7
		N 9	NA	1.5
		N10	NA	8.7
6	PI2	O 6	NA	25.7
		O 7	NA	59.3
		O 8	NA	0[a]
		O 9	NA	0[a]
		O10	NA	9.6

NA, not available
[a] These particles remained in a single hole of the free volume during the simulation time. These molecules were considered to be rather slow
[b] These particles jumped back and forth between two holes during the simulation time. The obtained D values are simply upper limits
[c] These particles moved up to 12.0 nm through one hole without limits in the x-axis direction. This behaviour is an artifact from the periodic boundary conditions and the limited model size. Therefore, the calculated constants of diffusion cannot be compared with the experimental data

'Snapshots' of the positions of all polymer and gas atoms were taken between every 250 and 1000 fs and saved in a history file.

Evaluation of data

The diffusion coefficient D and solubility S of small permeant molecules in polymers are among the most

Table 6 Free volume data from a topological prediction method[25,26]

Polymer	Van der Waals volume, V_v ($cm^3\ mol^{-1}$)	Molar volume at 0 K, V_0 ($cm^3\ mol^{-1}$)	Molar volume at 298 K, V_{298} ($cm^3\ mol^{-1}$)
PAI	295	418	443
PI1	340	472	498
PI2	414	585	618

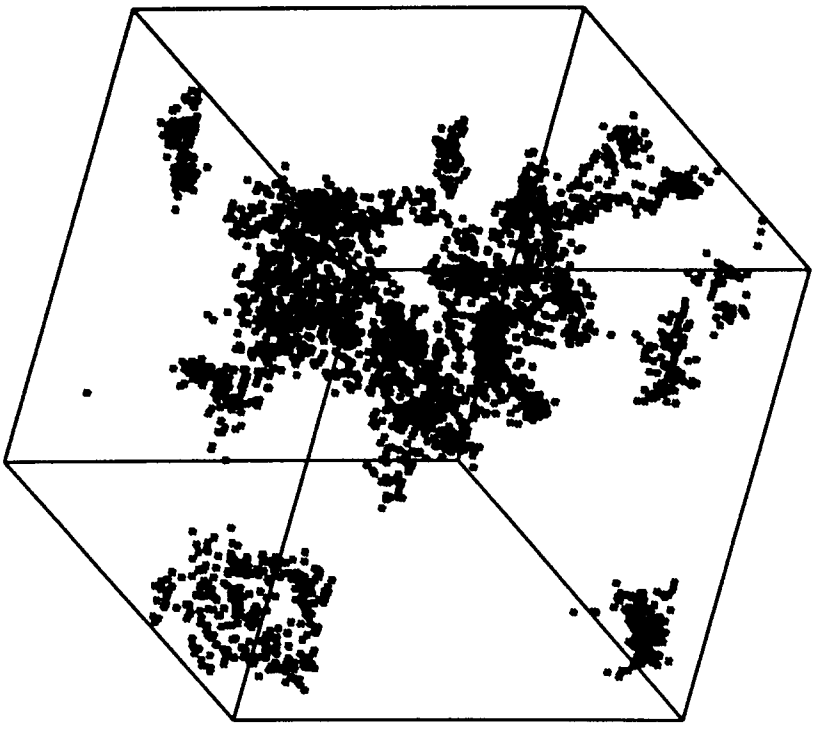

Figure 6 Free volume visited by the hydrogen molecules H10–H12 in PAI packing 4

interesting material parameters for gas separation. The permeability P for a gas that gives the quantity of gas permeating through a polymer film under standard conditions can then be obtained from

$$P = DS \tag{1}$$

In this paper the coefficient of diffusion for a gas molecule is calculated from the mean squared displacement $s(t) = \langle |R(t) - R(0)|^2 \rangle$ of this molecule averaged over all possible time origins $t = 0$ via the *Einstein* equation:

$$D = \langle |R(t) - R(0)|^2 \rangle / 6t \tag{2}$$

where R is the Cartesian position vector of a permeant molecule. A typical $\langle |R(t) - R(0)|^2 \rangle$ *versus* t plot is shown in *Figure 4*. A different approach was chosen in the cases of the permeant molecules H4 and H5 (see *Table 5*). These particles during the time of simulation mainly moved back and forth between two holes in the free volume, as can be concluded from the three peaks in the $\langle |R(t) - R(0)|^2 \rangle$ *versus* t curve shown in *Figure 5*. Such a behaviour will certainly also occur in reality, but there the particle will eventually (after sufficient time) reach other areas of the free volume. In those cases the diffusion coefficient can be roughly estimated using $D = \Delta s/(6\,\Delta t)$, with Δs and Δt being the average height and width of such a peak. The obtained D values are simply upper limits because the mentioned treatment assumes a straightforward movement through the sample that is usually not true in reality, where particles only on average proceed towards the permeate side of a membrane.

The Widom particle insertion method[28] was used to estimate the solubility S of a given gas in a polymer. S gives the concentration c of gas in a volume element of the polymer that is in equilibrium with an outside pressure reservoir of this gas. The results of the Widom method can be used in the content of equation (1) only for situations where Henry's law holds true. This means that the mentioned equilibrium concentration of a gas in a polymer is basically proportional to the pressure p. Henry's constant H is the constant of proportion in this case. The determination of S consists first of the insertion of virtual gas particles at random positions in a completely refined model polymer matrix followed by a calculation of the interaction energy E of such a particle with the polymer. Then the excess thermodynamic potential μ_{ex} is obtained via

$$\mu_{ex} = RT\ \ln\langle \exp(-E/kT) \rangle \tag{3}$$

S in turn is related to μ_{ex} by the following relation

$$S = \exp(\mu_{ex}/RT) \tag{4}$$

Table 7 Experimental and calculated solubilities

Packing No.	Polymer type	Gas type	Measured solubility, S_{exp} (bar^{-1})	Calculated solubility S_{calc} (bar^{-1})
1	PAI	H_2	0.114	1.266
		O_2	0.403	2640
		N_2	0.288	7600
2	PAI	H_2	0.114	0.497
		O_2	0.403	1650
		N_2	0.288	2060
3	PAI	H_2	0.114	0.797
		O_2	0.403	2040
		N_2	0.288	2520
4	PAI	H_2	0.114	0.978
		O_2	0.403	3320
		N_2	0.288	2890
5	PI1	H_2	NA	1.244
		O_2	2.16	3617
		N_2	1.65	2698
6	PI2	H_2	NA	0.945
		O_2	NA	900
		N_2	NA	2670

NA, not available

The basic Widom calculations were performed utilizing a FORTRAN program of Müller-Plathe[29], which was adapted to the conditions of the cvff by us.

A total of 20 000 particle insertions for each considered packing geometry was found to be sufficient to get stable S values for the simulated materials. A cut-off of 0.9 nm and the long-range correction given by Widom[28] were used for the energy calculations.

RESULTS AND DISCUSSION

Mechanism and diffusion coefficients

Usually only diffusion coefficients or $s(t)$ curves averaged over all (typically between three and 10) simulated permeant molecules are presented and discussed in the gas diffusion modelling literature. Due to the usually very restricted number of simulated gas molecules, we believe, however, that it is more instructive to consider the diffusion of each gas particle separately. *Table 5* contains the experimental and simulated values for the investigated gas molecules. A first look shows a considerable scattering of the calculated diffusion values that can be related to different modes of motion. There are gas particles (H3, H7, H9, N4, N7, O3, O8 and O9) which simply 'explored' the same hole in the free volume during the whole simulation time. Other

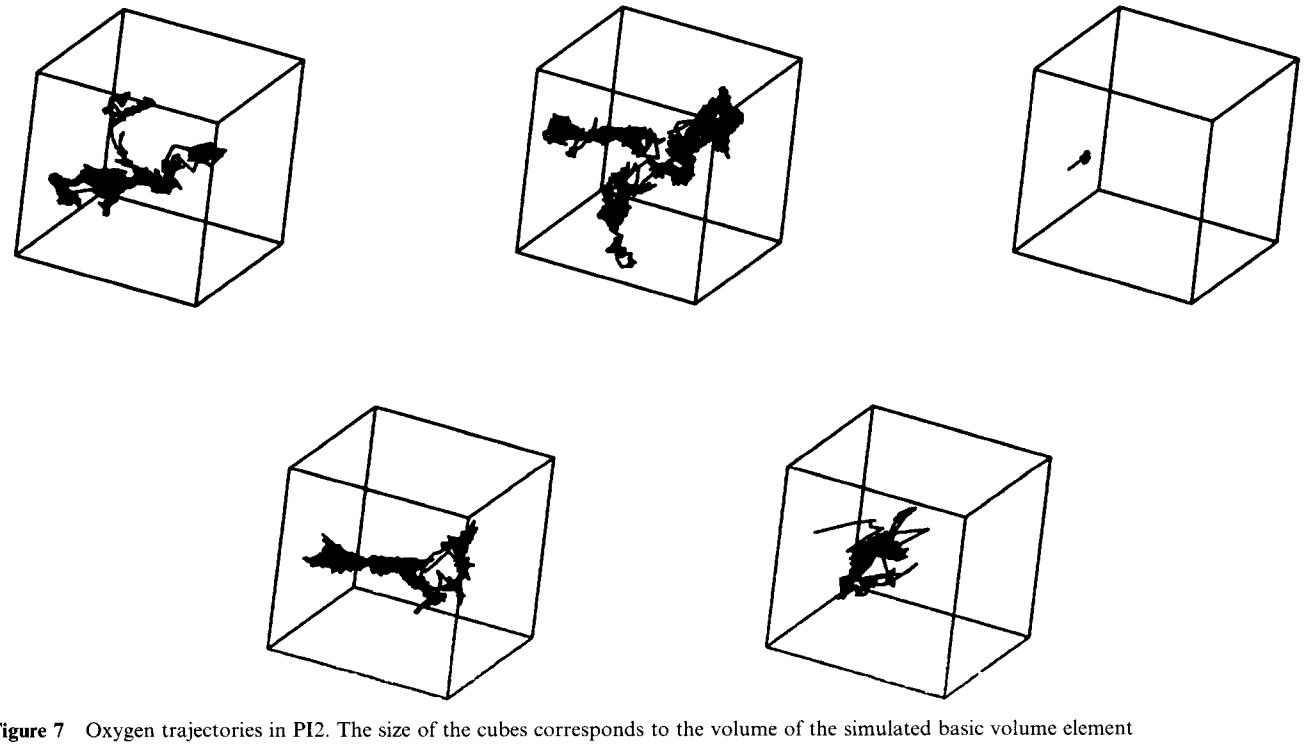

Figure 7 Oxygen trajectories in PI2. The size of the cubes corresponds to the volume of the simulated basic volume element

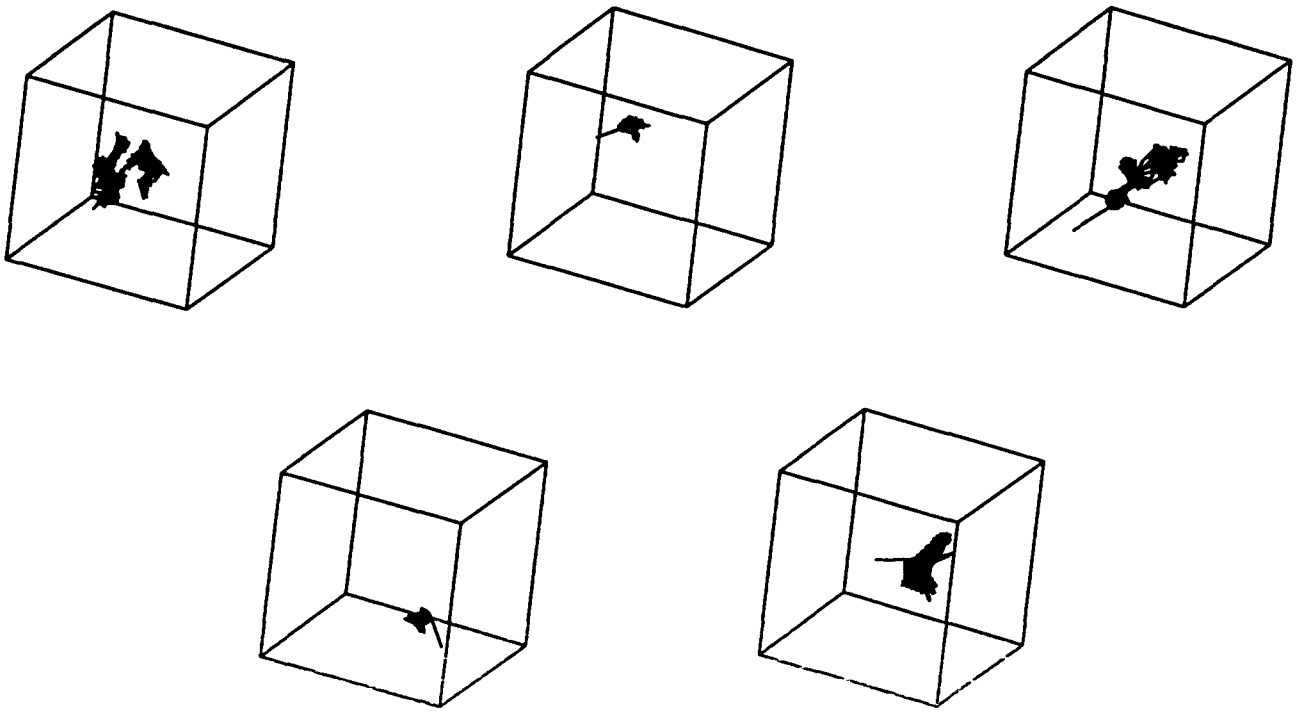

Figure 8 Nitrogen trajectories in PI2. The size of the cubes corresponds to the volume of the simulated basic volume element

molecules (H1, H2, H6, H8, N1–N3, N5, N6, N8–N10, O1, O2, O4–O7 and O10) revealed $s = s(t)$ curves which resembled the $s(t)$ functions averaged over several simulated particles that were reported in the literature (see *Figure 4*). (An evaluable positive slope of these $s(t)$ functions under the simulation conditions now possible can be found only in about the first two-thirds of the mean squared displacement function, while at higher t values this function becomes non-linear and noisy. This is a statistical effect resulting from the averaging over all possible time origins. It is therefore common practice[1–15] to discard the noisy tail of the $s(t)$ curve for the calculation of D values.)

As already mentioned in the last section, the hydrogen molecules H4 and H5 performed only jumps between the same two holes in the free volume during the simulation (see *Figure 5*). All the forementioned modes of motion may well also occur in real materials over the time-scale of the simulation (1–2.5 ns). The diffusion coefficients averaged over the molecules H1–H9, N1–N5, N6–N10, O1–O15 and O6–O10 each showed a factor of deviation from the experimental values well below 10 (see *Table 5*). These are values of deviation that were typically also observed in molecular simulations for more flexible chain polymers[1–15]. The correspondence of our average D values is, however, much better than reported for a CO_2 diffusion simulation in two polyimides by Smit *et al.*[16]. Thus, our simulation conditions are probably more realistic. The main reasons for this might be the considerably longer simulation times and considerably larger model sizes chosen by us. (The motion of H10–H12 was influenced by a simulation artifact that will be discussed below.)

A problem with D values obtained from the slope of $s(t)$ curves is the fact that these diffusion coefficients, though acceptable, are in most reported cases higher than in reality (see *Table 5* and the literature[1–15]). This seems partly to be related to the following fact. In the beginning of an MD diffusion simulation the first jump of each permeant molecule can simply lead away from its starting position (forward jump). If one could perform the simulation long enough (e.g. 100 ns in the given case) then the ratio between forward and backward jumps would be well balanced. For the simulation times (< 5 ns) that are common today there may be, however, a certain biasing of jumps leading clearly away from the origin of a particle. This, in turn, can be one cause of the mentioned overestimation of D values obtained via equation (2).

The so-called anomalous diffusion that was first reported by Müller-Plathe *et al.*[9,14] constitutes an additional problem for the calculation of D values from MD simulations. The Einstein equation (equation (2)) relies on the assumption of a random walk for each simulated particle through the polymer matrix. This means that the jumps of the gas molecules between individual holes in the free volume must determine the $s = s(t)$ behaviour. The rather short duration of MD simulations (up to 10 ns) does, however, result in a non-negligible influence of the very fast movement of permeant molecules (a time-scale of several hundred picoseconds) inside the individual holes on $s(t)$. This in-hole motion is determined by the shape of the holes, and is therefore not a random walk. The usual effect of anomalous diffusion is to create a somewhat smaller slope of the $s(t)$ curve at lower t values. The influence of this problem may extend up to several nanoseconds.

Another obstacle for accurate predictions of D values is the fact that in a real amorphous polymer each volume element shows a different packing of chain segments, while MD simulations can be performed only for a few packing cells. The problems mentioned so far indicate that much longer MD simulation times and many more different packing cells for each polymer–permeant system would be needed to obtain D values very close

to reality. This is outside the reach of the presently available hardware power, It is, however, possible to predict the order of magnitude of D for relatively fast diffusion processes, as can be seen from our investigation.

A newly developed transition state theory by Gusev and Suter[30–32] may be helpful for more exact predictions of the diffusion coefficient. There the diffusion of gas particles is simulated via a Monte Carlo-type procedure. The main advantage of this method is that much less CPU time is consumed, permitting much longer simulation times than MD. There is, however, a considerable loss in atomistic detail of the transport mechanism.

Another methodical problem has to do with the limited possible size of a packing cell. It is revealed by the extreme diffusion behaviour of the H_2 molecules H10, H11 and H12 of PAI packing 4 connected with up to 100 times higher D values than measured. The cause of this problem can be seen from *Figure 6*, which contains all the registered positions of H8–H12 projected in the original volume element during the simulation in PAI packing 3. These diagrams illustrate the shape of the free volume portions of the PAI packing that were explored by the gas particles between the jump events. It can be seen that H10–H12 move in a hole that extends from one side of the packing cell to the other. In such a case the hole is extended to infinity by the necessary periodic boundary conditions. This clear artifact of the simulation obviously permitted the very fast movement of the mentioned molecules. Obviously the obtained D values are physically meaningless in these cases. It should, however, be mentioned that voids with a length of 28 Å (length of packing cell 4) or more could certainly occur in reality. (The D values obtained for H10–H12 could be representative of a Knudsen diffusion of hydrogen in a hypothetical microporous PAI.)

Summarizing, it can be concluded that detailed atomistic MD simulations are, at least at the moment, not an ideal tool with which to predict diffusion coefficients of gas molecules in amorphous polymers. However, despite the mentioned problems the correspondence between simulated and measured diffusion coefficients is still acceptable. This indicates that some basic features of the gas diffusion process are correctly described by the simulations. It does, therefore, make sense to discuss the results of the MD investigations in more detail.

Figures 7 and *8* contain trajectories in the nitrogen and oxygen molecules in the PI2 packing. These trajectories, which are similar to the ones obtained for PI1, also show the shape of the visited free volume. It can be recognized that the gas particles are trapped in holes of rather defined shape for times between a few hundreds of picoseconds and the whole simulation time (up to 2.5 ns) before they eventually jump to an adjacent hole. Furthermore, the faster movement of oxygen as compared to nitrogen is clearly visible by the on average larger size of the visited matrix volume. The overall situation resembles results reported for MD simulations of gas transport in flexible chain polymers[1–15]. Typical mean squared displacement $s(t)$ and displacement $R(t)$ curves of oxygen are shown in *Figures 4* and *9*, respectively. These graphs give more quantitative information about the walk of a particle through the matrix material. There is again a striking similarity to the respective curves for flexible-chain polymers.

The simulated PAI, however, behaves in a different way. Here the free volume obviously consists of a smaller number of larger holes which are, in some cases, connected by a kind of more permanent channel, as can be seen from *Figure 10*. (A minor part of these geometric differences may be caused by the fact that the H_2 molecules simulated for the PAI are somewhat smaller than the O_2 and N_2 molecules utilized for PI1 and PI2.) As already discussed for H10–H12, this situation can even lead to holes being quasi-continuous over larger distances (see *Figure 6*). The larger hole size as compared with the PI results in the fact that for the PAI several gas particles are usually using the same set of holes for their diffusion (e.g. H4, H5, H6 and H10, H11, H12 in the holes shown in *Figures 10b* and *6*, respectively). The existence of more-permanent channels between holes may account for the observed much stronger tendency of repeated jumps of particles between the same two holes in the case of the PAI as compared with PI1 and PI2. This behaviour could also

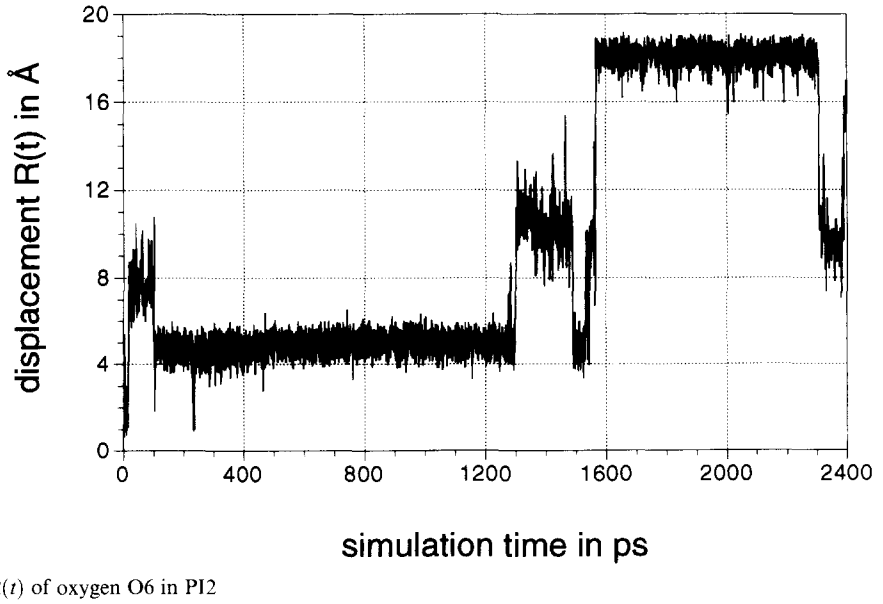

Figure 9 Displacement $R(t)$ of oxygen O6 in PI2

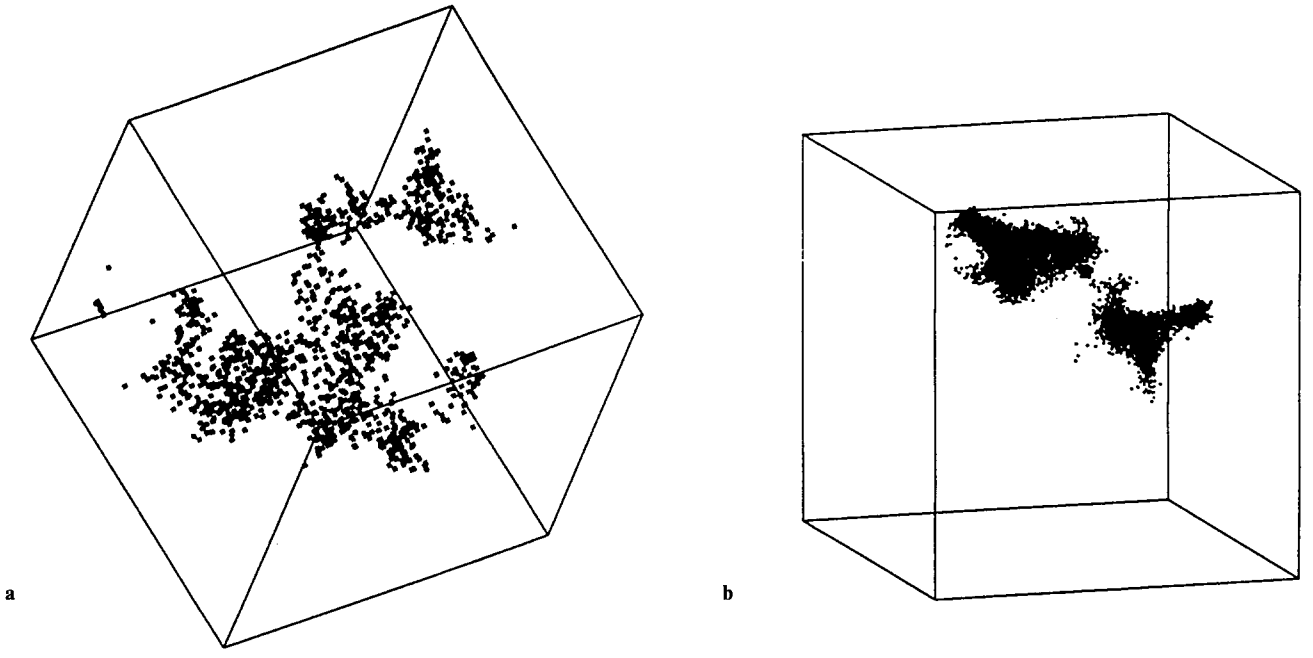

Figure 10 (a) Free volume visited by the hydrogen molecule H2 in PAI packing 2 (left side). (b) Free volume visited by the hydrogen molecules H4–H6 in PAI packing 3 (right side)

be a structural cause for the observed much smaller permeability and diffusivity values (see *Table 1*) of the PAI as compared to PI1 (and probably also PI3 and PI4).

A topological method developed by Bicerano[33,34] was utilized to estimate the van der Waals volume V_v and the molar volumes at 0 K (V_o) and 298 K (V_{298}) (*Table 6*). The relative content of free volume v_1, which is often calculated via[35]

$$v_1 = 1.3(V_v/V_{298}) \quad (5)$$

was about the same in all three cases, $v_f = 0.87, \ldots, 0.89$. (More generally, v_f is between V_v/V_{298}.) This consideration confirms that simple free volume concepts are often not sufficient for the discussion of differences in the diffusion behaviour.

Solubility

The experimental and calculated solubility values, S_{exp} and S_{calc}, respectively, are shown in *Table 7*. It must be stressed that the experimental S data were not obtained by sorption measurements, but calculated from the experimentally determined P and D values via $S = P/D$. Thus, S_{exp} simply describes the gas molecules solvated in the feed-side region of the polymer which actually take part in the diffusion process. According to the dual-mode sorption model (e.g. see Paul[36]), these molecules basically follow the Henry mechanism of sorption. The calculated data S_{calc}, however, consider both the gas particles showing a Henry behaviour and molecules following a Langmuir process.

For rubbers in general, and for small molecules (He, H_2) in amorphous polymers where a Henry sorption behaviour can be expected, simulated solubility values given in the literature are typically several times higher than the data measured in actuality[14]. Thus, it can be concluded from the S_{exp} and S_{calc} values given in *Table 7* that the hydrogen sorption in the PAI can be approximately described by Henry's law. Although no experimental data are available for the H_2 diffusion and sorption for H_2 in PI1 and PI2, the respective S_{calc} values seem to indicate a similar sorption mechanism.

The calculated solubilities for N_2 and O_2, however, are much higher than the experimental ones for both PI1 and the PAI. This may suggest that N_2 and O_2 tend to condense in the holes of the feed-side regions of these two polymers and PI2 following a Langmuir process. This means that a certain proportion of the solvated oxygen and nitrogen molecules does not take part in the diffusion process. Therefore, a dual-mode sorption model can be valid in these cases[36]. The extent of the discrepancy between S_{exp} and S_{calc} (resulting in a free energy deviation of some 20 kJ mol^{-1}) does, however, indicate that there are probably also contributions from technical problems such as, for example, the force field parameters used and/or microscopic density inhomogeneities.

CONCLUSIONS

The results presented suggest that molecular modelling techniques can be used to produce amorphous packings of the investigated PAI and PI materials that are sufficiently realistic on a length scale of about 3 nm. Furthermore, the diffusion behaviour of H_2, N_2 and O_2 could be acceptably simulated for time-scales of up to 2.5 nm. The diffusion process results from jumps of gas particles between adjacent holes as constituent parts of the free volume.

The free volume of PI1 and PI2 consists of a larger number of relatively small cavities. From time to time (about every few hundred picoseconds) relatively narrow channels between neighbouring holes are opened, through which the gas molecules can move. The lower diffusion coefficient of the nitrogen molecules as compared with oxygen is probably caused by the much stronger repulsive Lennard-Jones interactions for interatomic distances below about 0.38 nm (*Figure 11*) in the case of N_2. This prevents N_2 molecules more often than O_2

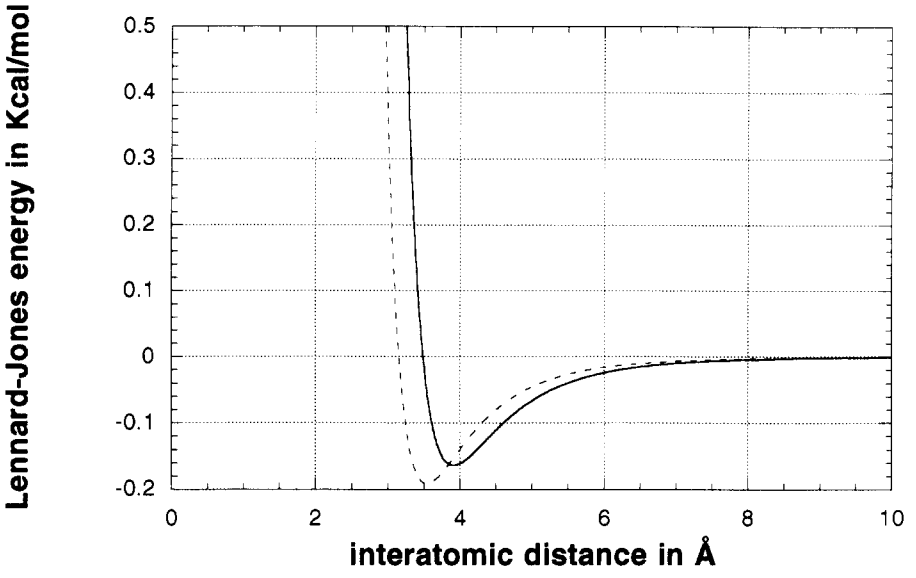

Figure 11 Lennard-Jones energies for oxygen–sp^3 carbon (solid line) and nitrogen–sp^3 carbon (dashed line) interactions

molecules from actually using an open channel for a jump.

The PAI, on the other hand, contains a smaller number of larger holes that are partly connected by slightly more permanent channels than in the case of the polyimides. This special character of at least some channels is a possible cause of the rather high rate of back and forth jumps between the same two holes observed for the PAI. The high rate of backward jumps in turn constitutes a major reason for the experimentally observed lower D values for H_2, N_2 and O_2 as compared with PI1. Therefore, in future research much more emphasis should be put on the nature of the channels than on the characteristics of the holes in amorphous polymers. In the case of the PAI the specific nature of the amide bonds, which are not present in PI1 and PI2, will, in particular, need further attention.

Detailed atomistic simulations are still not an ideal tool for the prediction of diffusion constants. (A possible though not completely satisfactory method for such a prediction was shown for the example PI2.) Here the first problem is that one still needs experimental density values to obtain reliable packing models. We tried to circumvent the problem in the case of PI2 by applying a very extensive packing equilibration procedure to this hypothetical polymer to obtain a reasonable guess about its density. In this case only the packing with the highest density that was stable during a 1 bar MD run was used for further investigation. Even more important, however, for the sake of good statistics and to avoid systematic errors such as anomalous diffusion, is that it would be necessary to improve the diffusion simulations in the following directions:

- much larger numbers of simulated packings (at least about 20);
- much larger overall numbers of simulated gas particles (up to several hundred for a whole set of simulations);
- much longer simulation times (often at least 100 ns).

Therefore, for predictive purposes, procedures also utilizing less atomistic detail should be used. These could be quantitative structure–property relationships (e.g. see Bicerana[33]) of a Monte Carlo type of approach such as the one proposed by Gusev and Suter[30–32].

The solubility considerations revealed a predominant Henry sorption mechanism for hydrogen in PI1, PI2 and the PAI. For oxygen and nitrogen, on the other hand, a dual-mode sorption model with a certain degree of Langmuir-type immobilization seems to be valid. It should, however, be mentioned that the influence of methodical problems on predicted solubility values such as the force field parametrization needs further attention.

Finally, it should be mentioned that the very similar simulation results for the experimentally available polymer PI1 and the hypothetical PI2 indicate only a minor influence of the additional trimethylphenylene group in PI2 on the gas diffusion mechanism. From the point of view of high-performance membrane development it seems, therefore, not to be necessary actually to perform the probably very laborious synthesis of PI2. However, it would certainly be interesting to compare the diffusion behaviour in real PI2 membranes with the *ab initio* simulation data for methodical reasons.

ACKNOWLEDGEMENTS

The authors are greatly indebted to Mrs C. Dannenberg and Mr M. Böhning, Institute of Technical Chemistry of the Technical University in Berlin, for the measurement of the diffusion coefficient for the PAI sample.

REFERENCES

1 Shah, V. M., Stern, S. A. and Ludovice, P. J. *Macromolecules* 1989, **22**, 4660
2 Sok, R. M. and Berendsen, H. J. B. *Polym. Prepr.* 1992, **33**, 641
3 Trohalaki, S., Rigby, D., Kloczowski, A., Mark, J. E. and Roe, R. J. in 'Computer Simulations of Polymers' (Ed R. J. Roe), Prentice Hall, Englewood Cliffs, NJ, 1991, p. 220
4 Takeuchi, H. and Okazaki, K. *J. Chem. Phys.* 1990, **92**, 5643
5 Sonnenburg, J., Gao, J. and Weiner, J. H. *Macromolecules* 1990, **23**, 4653
6 Boyd, R. H. and Krishna Pant, P. V. *Macromolecules* 1991, **24**, 6325

7 Krishna Pant, P. V. and Boyd, R. H. *Macromolecules* 1993, **26**, 679
8 Sok, R. M., Berendsen, H. J. C. and van Gunsteren, W. F. *J. Chem. Phys.* 1992, **96**, 4699
9 Müller-Plathe, F., Rogers, S. C. and van Gunsteren, W. F. *Chem. Phys. Lett.* 1992, **199**, 237
10 Takeuchi, H. *J. Chem. Phys.* 1990, **93**, 2062
11 Müller-Plathe, F. *J. Chem. Phys.* 1991, **94**, 3192
12 Müller-Plathe, F. *J. Chem. Phys.* 1992, **96**, 3200
13 Krishna Pant, P. V. and Boyd, R. H. *Macromolecules* 1992, **25**, 494
14 Müller-Plathe, F. *Acta Polym.* 1994, **45**, 259
15 Gusev, A. A., Müller-Plathe, F., van Gunsteren, F. W. and Suter, U. W. *Adv. Polym. Sci.* 1994, **16**, 207
16 Smit, E., Mulder, M. H. V., Smolders, C. A., Karrenbend, H., van Eerden, J. and Feil, D. *J. Membrane Sci.* 1992, **73**, 247
17 Dauber-Osguthorpe, P., Roberts, V.-A., Osguthorpe, D. J., Wolff, J., Genest, M. and Hagler, A. T. *Proteins: Structure, Functions Genetics* 1986, **4**, 82
18 Hayes, R. A. US Pat. 4,705,540, 1987
19 Fritsch, D. and Peinemann, K.,-V. *J. Membrane Sci.* 1995, **99**, 29
20 'Discover User Guide', Version 2.3.5, Biosym Technologies, San Diego, 1994
21 Hagler, A., Lifson, S. and Dauber, P. *J. Am. Chem. Soc.* 1979, **101**, 5122
22 Hagler, A., Lifson, S. and Dauber, P. *J. Am. Chem. Soc.* 1979, **101**, 5131
23 Theodorou, D. N. and Suter, U. W. *Macromolecules* 1985, **18**, 1467
24 Theodorou, D. N. and Suter, U. W. *Macromolecules* 1986, **19**, 139
25 'Polymer User Guide', Version 6.0, Amorphous Cell Section, Biosym Technologies, San Diegeo, 1993
26 Flory, P. J. 'Statistical Mechanics of Chain Molecules', Hanser, 1989
27 Berendsen, H. J. C., Postma, J. P. M. van Gunsteren, W. F., DiNola, A. and Haak, J. R. *J. Chem. Phys.* 1984, **81**, 3684
28 Widom, B. J. *Chem. Phys.* 1963, **39**, 2808
29 Müller-Plathe, F. personal communication (FORTRAN program widom2)
30 Gusev, A. A., Arizzi, S. and Suter, U. W. *J. Chem. Phys.* 1993, **99**, 2221
31 Gusev, A. A. and Suter, U. W. *J. Chem. Phys.* 1993, **99**, 2228
32 Gusev, A. A. and Suter, U. W. *Computer-aided Mat. Design* 1993, **1**, 63
33 Bicerano, J. 'Prediction of Polymer Properties', Marcel Dekker, 1993
34 'Polymer User Guide', Version 6.0, Synthia Section, Biosym Technologies, San Diego, 1993
35 Hensema, E. R., Mulder, M. H. V. and Smolders, C. A. *J. Appl. Polym. Sci.* 1993, **49**, 2081
36 Paul, D. R. *Ber. Bunsenges. Phys. Chem.* 1979, **83**, 294

NOTE ADDED IN PROOF

Recent investigations of the authors on the determination of solubility values for the investigated PAI and PII packing models utilizing the Gusev–Suter method and the Biosym pcff force-field have produced a much better coincidence between measured and simulated values than reported in this paper. The respective values of the PAI packing 2, for instance, are $0.10\,bar^{-1}$, $1.24\,bar^{-1}$ and $0.54\,bar^{-1}$ for H_2, O_2 and N_2, respectively. Since, in principle, the Gusev–Suter method should produce the same solubility values as the Widom technique, the pcff force-field is obviously much better suited for this kind of calculation. The problem with cvff seems to consist of the specific implicit consideration of hydrogen bonds via manipulated Lennard-Jones and electrostatic terms used for this force-field. Since the utilized solubility calculations do not consider electrostatic terms, severe systematic errors may arise for polymers containing atoms capable of forming hydrogen bonds. Details of these new investigations will be given in a subsequent paper.